Published online May 13, 2005

Scaling and Estimation of Evaporation and Transpiration of Water across Soil Textures

Joseph A. Kozak,* Lajpat R. Ahuja, Liwang Ma, and Tim R. Green

ABSTRACT

A recent study showed all parameters in the Brooks-Corey equations of soil hydraulic properties are strongly correlated to the pore-size distribution index (λ). These λ values relate and can scale cumulative infiltration and water contents during redistribution across dissimilar textural classes under different rainfall and initial conditions. The objectives of this work were to explore if relationships exist between evaporation (*E*) and transpiration (*T*) and λ across different soil types and if these relationships can be used to scale *E* and *T* among these soils. The Root Zone Water Quality Model generated evaporation under four potential rates and transpiration under one potential rate with a goosegrass [*Eleusine indica* (L.) Gaertn.] in 11 soil textural classes under near-saturated initial conditions. Stage I cumulative evaporation or transpiration that occurs when the soil is sufficiently wet to meet the potential rates had a quadratic relationship with λ. However, both Stage II cumulative evaporation and transpiration were cubic functions of λ with time-dependent coefficients. It is shown that these relationships can be used to estimate both Stage I and II cumulative evaporation and transpiration across unknown soils, especially when data for one dominant reference soil type is known. The methods developed for estimating cumulative evaporation were applied and compared with experimental results of three initially saturated soils under constant evaporation with good results. These results for simple homogeneous soils should be useful in quantifying spatial variability of evaporation and transpiration in the field under similar conditions, and could form the basis for further research of more complex conditions.

Scaling has been used as a tool for approximately describing field spatial variability of soil hydraulic properties—matric potential and unsaturated hydraulic conductivity as a function of soil water content (e.g., Warrick et al., 1977; Simmons et al., 1979; Russo and Bresler, 1980) as well as characteristics derived from these, such as the infiltration (Sharma et al., 1980). The frequency distribution and spatial-correlation structure of scaling factors describe variability in the field, thus resulting in considerable simplicity and enhanced understanding as well as convenience in modeling a heterogeneous watershed for its hydrologic responses (Pachepsky et al., 2003; Nielsen et al., 1998; Peck et al., 1977; Sharma and Luxmoore, 1979; Warrick and Amoozegar-Fard, 1979; Ahuja et al., 1984). Inversely, scaling can also be used to estimate soil hydraulic properties at different locations in a watershed from measurement of these properties at one representative location and limited data at other locations (Ahuja et al., 1985; Williams and Ahuja, 1991).

Two methods to derive the scaling factors are well-known (Tillotson and Nielsen, 1984): (i) the dimensional analysis technique, which is based on the existence of physical similarity in the system; and (ii) the empirical method, called functional normalization, which is based on regression analysis. The similar-media scaling of Miller and Miller (1956) and the fractal-based approaches of Tyler and Wheatcraft (1990), Rieu and Sposito (1991), and Hunt and Gee (2002) are examples of the first method. Most of the scaling work cited above has extended the similar-media scaling concept to field soils that are generally "nonsimilar" by invoking additional empirical assumptions and using a regression method.

Very limited research has been done on relating soil hydraulic properties across widely dissimilar soil textural classes. Gregson et al. (1987) showed that the slope and intercept of the commonly used Brooks and Corey (1964) log-log relationship for soil matric potential–water content function, below the air-entry value, were highly correlated across 41 Australian and British soil classes. This formed the basis for their one-parameter model for estimating the soil water retention curve in any soil. In a recent book chapter, Williams and Ahuja (2003) showed that: (i) there was a strong relationship between the intercepts and slopes of textural class mean water retention curves (obtained from using the geometric mean Brooks-Corey parameters) for 11 U.S. soil classes from sand to clay (Rawls et al., 1982); and (ii) these curves could be scaled very well (brought together closely) using their slopes as scaling factors. More recently, Kozak and Ahuja (2005) found that K_s and even the air-entry or bubbling pressures of these textural class mean curves had a strong logarithmic relation with their slopes. The air-entry value on the log-log water retention curve defined by the slope–intercept relation also determines the saturated soil water content.

Further, if we accept the assumption that the unsaturated hydraulic conductivity curve can be estimated from the known water retention curve, and K_s value, as established by numerous investigations (See Campbell, 1974; Green et al., 1982) and used commonly by modelers, the slope of the log-log water retention curve can be used to estimate the conductivity curve as well. Thus, the slope of the water retention curve (pore-size distribution index, λ) determines both the soil hydraulic properties instrumental in soil water movement.

Kozak and Ahuja (2005) showed that λ could be used to normalize and scale infiltration across textural classes under several rainfall intensities, based on the Green and Ampt (1911) model. They also derived strong empirical relationships of infiltration and soil water content changes during subsequent redistribution with λ values for the 11 textural classes. These relationships could be used to

USDA-ARS-NPA-GPSR, 2150 Centre Ave., Bldg. D, #2055, Fort Collins, CO 80526-8119. Received 10 Aug. 2004. Original Research Paper. *Corresponding author (joseph.kozak@ars.usda.gov).

Published in Vadose Zone Journal 4:418–427 (2005).
doi:10.2136/vzj2004.0119

677 S. Segoe Rd., Madison, WI 53711 USA

Abbreviations: LAI, leaf area index; PE, potential evaporation; PET, potential evapotranspiration; PT, potential transpiration; RMSE, root mean square errors; RZWQM, Root Zone Water Quality Model.

Table 1. Hydrological properties of 11 textural classes.

Soil textural class	Total porosity, θ_s	Geometric mean bubbling pressure, $\lvert\psi_b\rvert$	Residual saturation, θ_r	Geometric mean pore size distribution, λ	Saturated hydraulic conductivity
	$m^3\ m^{-3}$	kPa	$m^3\ m^{-3}$		$cm\ h^{-1}$
Sand	0.437	0.726	0.02	0.591	21.00
Loamy sand	0.437	0.869	0.035	0.474	6.11
Sandy loam	0.453	1.466	0.041	0.322	2.59
Loam	0.463	1.115	0.027	0.22	1.32
Silt loam	0.501	2.076	0.015	0.211	0.68
Sandy clay loam	0.398	2.808	0.068	0.25	0.43
Clay loam	0.464	2.589	0.075	0.194	0.23
Silty clay loam	0.471	3.256	0.04	0.151	0.15
Sandy clay loam	0.430	2.917	0.109	0.168	0.12
Silty clay loam	0.479	3.419	0.056	0.127	0.09
Clay	0.475	3.73	0.09	0.131	0.06

estimate infiltration and soil water contents across textural classes.

The amount of actual evaporation or crop transpiration from a soil system are controlled by atmospheric demand, as well as the available water content, and the soil water movement to meet this demand. The latter is a function of soil hydraulic properties. Thus, we expect that for a given potential evaporation or transpiration demand, the actual evaporation or transpiration among different soil types will be related to their λ values. The objectives of this research were: (i) to explore any direct explicit relationships among λ values and evaporation and transpiration of soil water with time; and (ii) to use these explicit relationships to scale or estimate evaporation and transpiration across different soil textures. This knowledge will help to understand and estimate spatial variability of evaporation and transpiration over large vegetated and unvegetated areas, which are most often the cause of spatial variability in soil water content and crop yield, and hopefully to devise site-specific management. The knowledge will also help in scaling up evaporation and transpiration predictions from small plots to fields and watershed levels, knowing the distribution of soils.

MATERIALS AND METHODS

Table 1 gives the geometric mean Brooks and Corey (1964) hydrological parameters for water retention and saturated hydraulic conductivity for 11 textural classes ranging from sand to clay (Rawls et al., 1982). These parameters were based on 1323 soils with approximately 5350 horizons compiled from data of nearly 400 soil scientists. Using these parameters, hypothetical studies examining the evaporation and transpiration of water across textural classes were performed through the implementation of the Root Zone Water Quality Model (RZWQM) (Ahuja et al., 2000; Ma et al., 2002). The USDA Agricultural Research Service's RZWQM is an integrated physical, biological, and chemical process model that simulates plant growth and movement of water, nutrients, and pesticides over and through the root zone at a representative area of an agricultural cropping system (Ahuja et al., 2000). Evaporation and transpiration were simulated as follows.

Evaporation Simulations

In RZWQM, soil evaporation is determined by soil water movement to the soil surface as determined by the Richards' equation and its boundary conditions. For evaporation, the upper boundary conditions in the simulations were a constant potential evaporation rate until the pressure head at the soil surface reached −1500 kPA, followed by a constant head (−1500 kPa) and declining evaporation rate dependent on water availability. The potential evaporation rates in each scenario are maintained in Stage I as there is enough available water in the soil profile to meet the evaporative demand, after which (Stage II) the declining actual rates of soil evaporation are controlled by the soil water movement to the surface (Ritchie, 1972). The lower boundary condition was a unit hydraulic gradient, namely free gravity flow, for all scenarios.

For each textural class, four bare soil evaporation scenarios were simulated for 34 d under four potential evaporation rates (Table 2). The soil profile for each simulation was homogeneous and 300 cm deep. The entire profile was assumed initially wetted by a rainfall or irrigation event to field saturation, namely 90% of full saturation; field saturation is the most common initial condition for evaporation or transpiration. It should be noted that although all 11 textural classes have the same initial degree of water saturation, the corresponding initial pressure heads may vary. We did not consider a shallower wetting depth, a lower initial degree of saturation, or higher soil water contents for this study; these conditions may influence results and may be studied in the future. A field-saturated profile for all studied soils assured that both stages of evaporation and transpiration would occur. Input parameters for the evaporation study are summarized in Table 2.

Transpiration Simulations

In RZWQM, the root water uptake function of Nimah and Hanks (1974) acts as a sink term in the Richards' equation at different depths of the root zone, and the sum total of uptake determine the actual rates of crop transpiration with upper limits defined by the potential transpiration rates. In the model, the effective root water pressure head is adjusted during simulation to meet the transpiration demand. This root water pressure head is not allowed to go below −1500 kPa; after it reaches −1500 kPa, it is maintained at this value, and the transpiration falls below the potential. It is noted that this pressure head minimum may be higher for some crop species,

Table 2. Input parameters for RZWQM evaporation study.

Parameter	Value
Simulation time	34 d
Depth of soil profile	300 cm
Depth of wetted profile	300 cm
Degree of saturation	0.90
PE (potential evaporation)	0.3 cm d^{-1} (scenario 1)
	0.5 cm d^{-1} (scenario 2)
	0.7 cm d^{-1} (scenario 3)
	1.0 cm d^{-1} (scenario 4)

Table 3. Input parameters for RZWQM transpiration study.

Parameter	Value
Simulation time	60 d
Depth of soil profile	300 cm
Depth of wetted profile	300 cm
Degree of saturation	0.90
Vegetation	goosegrass
Leaf area index	8.0
Total seasonal N uptake	50 kg ha^{-1}
Stover produced at cutting	2000 kg ha^{-1}
C/N ratio of stover	50.0
PET (potential evapotranspiration)	0.5 cm d^{-1}
Actual evaporation	~0.005 cm d^{-1}
Crop height	40 cm
Rooting depth	100 cm

but in general, −1500 kPa can be used for most crops. The lower boundary condition was a unit hydraulic gradient.

For each textural class, a single transpiration scenario was simulated for 60 d using RZWQM's simple Quickturf option; the soil system included a mature goosegrass with a leaf area index (LAI) of 8.0 (Table 3). The soil profile for each simulation was homogeneous and 300 cm deep. The entire profile was assumed initially wetted by a rainfall or irrigation event to field saturation. Daily potential evapotranspiration (PET) rate of 0.5 cm d^{-1} was partitioned into potential evaporation (PE) and potential transpiration (PT) according to the Shuttleworth-Wallace (1985) methods employed in RZWQM. Because of the high goosegrass coverage and maturity of the vegetation imposed during the model simulation, the evaporation from the soil surface was greatly minimized and was essentially negligible; therefore, PT essentially equaled PET. Like the evaporation experiment, the soil system maintained the PT rate in Stage I, after which the actual rates of transpiration rates are determined by the maximum rates of the soil water movement to plant roots. In the Quickturf option, root density assumes diamond-shaped distribution in the soil profile, where the maximum root density is highest at the middle depth (50 cm) and lowest at the top and bottom of the profile (0 and 100 cm, respectively). Additionally, using the Quickturf option removes any stress. The vegetation used in the simulation was assumed mature; the LAI, root distribution, root depth, and other plant physical characteristics were constant throughout the simulation. Input parameters for the transpiration study are summarized in Table 3.

Methods for Relating Evaporation to λ

The duration and magnitude of Stage I and the actual rates in Stage II vary with soil textural classes and their hydraulic properties. The upward movement of soil water to the soil surface due to evaporative flux in both stages and the downward movement of soil water out of the evaporation zone are controlled by the soil hydraulic properties. Because of this, we expect the total evaporation in Stage I (E_{s1}) and evaporation rates in Stage II to be related to soil λ values.

Upon simulation of the scenarios summarized in Table 2, the Stage I evaporation results for the 11 textural classes were examined with respect to their λ values. The simulated results indicated a trend of a quadratic relationship between log cumulative Stage I evaporation, CE_{s1}, and log λ. The possible reasons for this form of relationship will be discussed in the Results and Discussion section. Thus, for a specific potential evaporation rate, a generalized equation for CE_{s1} as a function of λ, was hypothesized,

$$\log CE_{s1} = A(\log \lambda)^2 + B(\log \lambda) + C \quad [1]$$

where CE_{s1} is an explicit function of a single parameter λ, and A, B, and C are fitted empirical coefficients.

Log-log plots of CE_{s1} vs. λ for the mean homogeneous soils of 11 textural classes for PE of 0.3, 0.5, 0.7, and 1.0 cm d^{-1} and the initial conditions summarized in Table 2 were made. The empirical coefficients mentioned determined for each scenario were explored for their relationship to varying PE rates. For a given λ, direct relationships between CE_{s1} and PE rates were also explored.

The simulated data indicated a curvilinear cubic relationship trend observed between the log cumulative Stage II evaporation, CE_{s2}, and log λ. Thus, for a specific PE rate, a generalized equation for CE_{s2} as a function of λ, was hypothesized as follows:

$$\log CE_{s2} = a(\log \lambda)^3 + b(\log \lambda)^2 + c(\log \lambda) + d \quad [2]$$

where the parameters a, b, c, and d are empirical coefficients. Daily log-log plots of CE_{s2} vs. λ for the mean homogeneous soils of 11 textural classes for all four PE rates were made for 2 wk after initiation of Stage II evaporation. The empirical coefficients (a–d) mentioned above were determined for each scenario and each day.

Experimental Data for Comparison

Bonsu (1997) performed an evaporation study on 10 saturated bare soils of different textures. These soils were subjected to a constant evaporation rate of 1.0 cm d^{-1} by direct sunshine during the day and by a fan during the night in the laboratory. The cumulative depth of evaporation was measured daily for a period of 2 wk. Stage I and II evaporations from these data were compared with results estimated from λ-based relations.

Methods for Relating Transpiration to λ

Much like evaporation, this study assumes two stages of transpiration, the constant and falling rate stages. In the constant rate stage, T_1, the soil is sufficiently wet for the water to be extracted by the plant roots at a rate equal to that of the transpiration potential. In the falling stage, T_2, the soil water content has decreased below a threshold value, so that transpiration depends on the flux of water to the roots. Relationships of T_1 and T_2 transpiration with λ were explored only for one potential rate of 0.5 cm d^{-1}.

The simulated results indicated a quadratic trend or relation between log cumulative Stage I transpiration, CT_1, and log λ. Thus, an equation similar to Eq. [1] was hypothesized for CT_1 as follows:

$$\log CT_1 = D(\log \lambda)^2 + E(\log \lambda) + F \quad [3]$$

where D, E, and F are fitted empirical coefficients. Log-log plots of cumulative Stage I transpiration, CT_1 vs. λ for the mean homogeneous soils of 11 textural classes were made from the RZWQM simulated results of the 0.5 cm d^{-1} transpiration scenario (Table 3).

The simulated data indicated a trend of a curvilinear cubic relationship between log cumulative Stage II transpiration, CT_2, and log λ. Thus, for a specific PT rate, a generalized equation for CT_2, as a function of λ, was hypothesized as follows:

$$\log CT_2 = e(\log \lambda)^3 + f(\log \lambda)^2 + g(\log \lambda) + h \quad [4]$$

where the parameters, e–h, are fitted coefficients. A log-log plot of CT_2 vs. λ for the mean homogeneous soils of 11 textural classes was made for 2 wk on initiation of Stage II transpiration. The empirical coefficients (e–h) mentioned above were determined for each day.

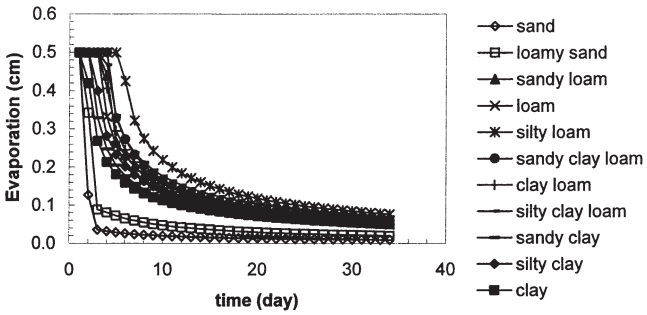

Fig. 1. Plot of simulated evaporation and time for a PE of 0.5 cm d^{-1}.

RESULTS AND DISCUSSION

Evaporation Relationships

A plot of actual daily soil evaporation, E_s, and time is shown in Fig. 1 for all 11 textural classes for the 0.5 cm d^{-1} potential evaporation rate scenario. The plot exhibits both stages of evaporation. Log-log plot of cumulative Stage I evaporation (CE_{s1}) for three PE rates vs. the pore-size distribution index of each soil are shown in Fig. 2. A quadratic curve is fitted to the raw data using Eq. [1] with r^2 values of 0.69 to 0.76. The scatter in the relation may be due to the fact that λ does not perfectly relate to soil hydraulic properties. In Fig. 2, the Stage I evaporation initially increases with increase in λ, reaches a plateau, and then decreases with further increase in λ. The pattern of the relationship has to be caused by the rates of changes in soil water content due to downward movement with time as well as evaporation and the corresponding changes in unsaturated hydraulic conductivity (K) near the soil surface in different soil types. For clay and clay loam soils (small λ values), the unsaturated hydraulic conductivity is very low. For the sandy loam, loamy sand, and sand soils (large λ values), very fast drainage of the surface water results in a rapid decrease in unsaturated hydraulic conductivity due to large λ values. For loam soils (middle range of λ values), the unsaturated K remains high.

The empirical coefficients A and B in Fig. 2 were linearly related to PE rate, whereas coefficient C had a

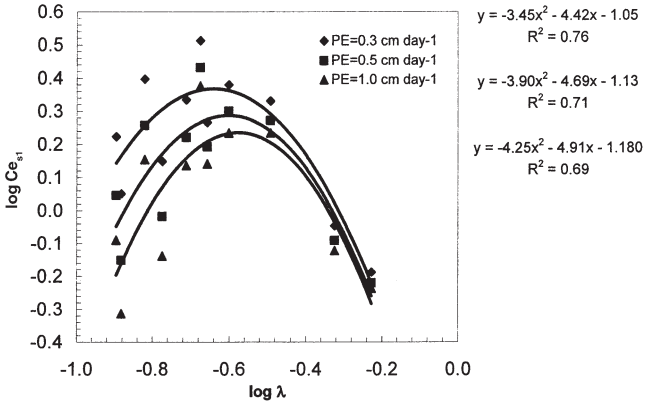

Fig. 2. Log-log relationship of the pore-size distribution index (λ) and computed cumulative Stage I evaporation (CE_{s1}) for the 11 textural-class mean soils for three PE rates.

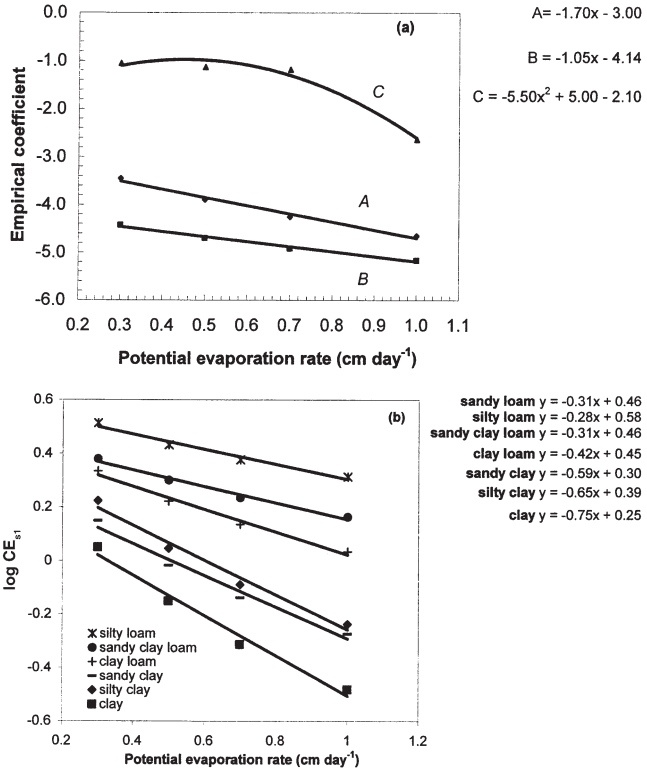

Fig. 3. (a) Plot of the empirical coefficients of Eq. [2] and potential evaporation rates for cumulative Stage I evaporation; and (b) plot of log CE_{s1} and potential evaporation rates for cumulative Stage I evaporation for representative soils.

quadratic relationship (Fig. 3); the latter curve was determined to have the best fit. These equations can be used to find the value of the empirical coefficients for any potential evaporation rate. Substituting these empirical coefficient values into Eq. [1] will give an estimate of the cumulative Stage I evaporation for any soil with a known λ. Additionally, a direct plot of log CE_{s1} vs. the four PE rates for seven soils covering the entire range of textural classes indicated a high correlation but a decreasing linear trend with λ (Fig. 3b). These results are interesting, as the linear regression lines fitted to the raw data can also be used to estimate CE_{s1} for any soil type. Table 4 gives the linear equations for all 11 textural classes.

A log-log plot of cumulative Stage II evaporation, CE_{s2} vs. λ is shown in Fig. 4a and 4b for the 0.5 cm d^{-1} PE rate. (Note: Not all times are shown to avoid confusion; however, all absent times, t_2, were observed to follow

Table 4. Cumulative Stage I evaporation linear equations as a function of potential evaporation for all 11 textural mean classes.

Soil textural class	CE_{s1} linear equations
Sand	$-0.13(PE) - 0.15$
Loamy sand	$-0.13(PE) - 0.02$
Sandy loam	$-0.32(PE) + 0.46$
Loam	$-0.27(PE) + 0.34$
Silty loam	$-0.28(PE) + 0.58$
Sandy clay loam	$-0.31(PE) + 0.46$
Clay loam	$-0.42(PE) + 0.45$
Silty clay loam	$-0.51(PE) + 0.53$
Sandy clay	$-0.59(PE) + 0.30$
Silty clay	$-0.65(PE) + 0.39$
Clay	$-0.75(PE) + 0.25$

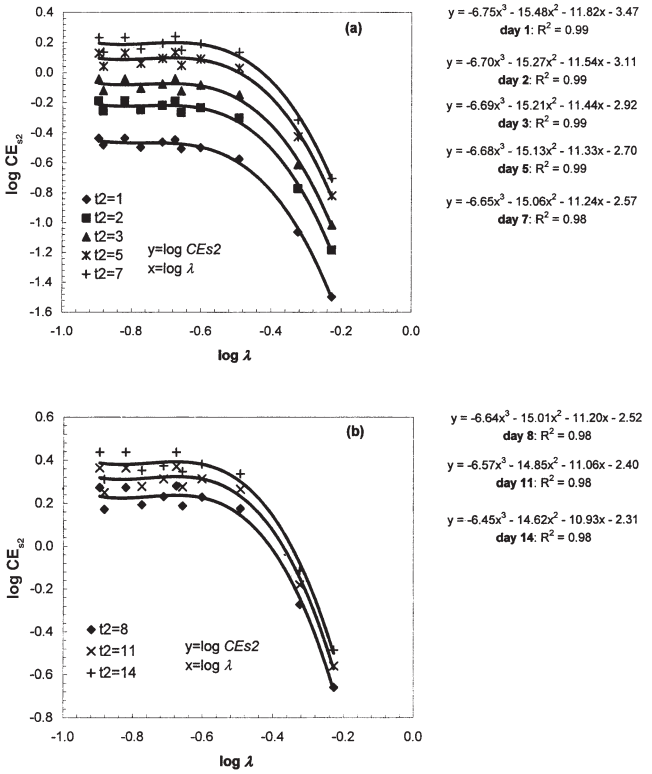

Fig. 4. (a) Log-log relationship of the pore-size distribution index (λ) and computed cumulative Stage II evaporation (CE_{s2}) for the 11 textural-class mean soils for a PE of 0.5 cm d^{-1}, for various times, t_2, ranging from 1 d (bottom curve) to t_2 = 7 d (top curve). Cubic equations are fitted to cm data for each day; and (b) log-log relationship of the pore-size distribution index (λ) and computed cumulative Stage II evaporation (CE_{s2}) for the 11 textural-class mean soils for various times, t_2, ranging from 8 to 14 d for a PE of 0.5 cm d^{-1}.

the same trend as the times presented.) As indicated from the r^2 values close to unity (0.98–0.99 for t_2 = 1–7 and 0.97–0.98 for t_2 = 8–14), a strong relationship exists between CE_{s2} and λ. It is observed in Fig. 4a and 4b that the CE_{s2} trend line is curvilinear and descends as the λ values increase. These higher λ values are associated with the coarser-textured soils, such as sand, loamy sand, and sandy loam. Because of the higher saturated hydraulic conductivities of these coarser soils, the soil profile is able to drain rather quickly, thus leaving less water in the system compared with the finer soils. Therefore, there is less actual evaporation in a soil profile that has less water available for potential evaporation and has lower unsaturated conductivities. Equation [2] fitted well to the simulation results for each potential evaporation rate.

Evaporation Scaling

For quick approximate scaling and estimation of results for unknown soils from known results for a reference soil, we further hypothesized that the log CE_{s2}–log λ plots for different PE rates may be approximated as parallel, for example Fig. 4a and 4b, although there were some deviations in the simulated data. Using a single reference time (t_{ref}) and applying the cubic regression equation for log CE_{s2}–log λ, estimated (e) values of each soil's cumulative Stage II evaporation at that time can be computed, CE^e_{2i}. These estimated cumulative Stage II evaporation values are then compared with the estimated value of a reference soil, CE^e_{2ref}. The difference between the two variables gives a scaling factor, α_i, for the respective soil,

$$\alpha_i = \log CE^e_{2i} - \log CE^e_{2ref} \quad [5]$$

With these scaling factors, predictions of the actual depth of cumulative Stage II evaporation for each soil can be made, given that the cumulative Stage II evaporation for the reference soil, CE_{2ref}, is known (Method IA).

$$\log CE_{2i} = \log CE_{2ref} + \alpha_i \quad [6]$$

The scaled values calculated for all evaporation scenarios through Eq. [6] uses loam as the reference soil, whose λ (= 0.220) was close to the mean of all λ values. Because the evaporation study was conducted for a period of 2 wk, a t_{ref} of Day 4 for the 1- to 7-d time span and Day 11 for the 8- to 14-d time span were used. Five soils were examined (sand, loamy sand, sandy loam, sandy clay, and clay) to encompass the entire range of soil textural classes (Rawls et al., 1982). However, it should be noted that any soil of known λ can be used as the reference, and any time of interest within the 14-d period can be used as t_{ref}.

The RZWQM simulated CE_{s2} values for the five of the soils encompassing the range of soil textural classes were compared with the scaled values for each respective soil. The scaling results (Eq. [5] and [6]) using the empirical coefficients at t_{ref} = 4 d and t_{ref} = 11 d from the cubic equations in Fig. 4a and 4b for the 0.5 cm d^{-1} evaporation rate scenario are shown in Fig. 5a and 5b. As can be seen, there is good agreement between the simulated and scaled log values of CE_{s2} for each soil over time. Discrepancies between the simulated and scaled results may be due to the imperfect log CE_{s2}–log λ relationship and approximate nature of the method.

The same scaling approach was applied with respect to the soil systems with three more potential evaporation rates of 0.3, 0.7, and 1.0 cm d^{-1} to examine the effect of the upper boundary condition on scaling. The r^2 values based on the cubic function fitted for the raw data of the log-log plots of CE_{s2} vs. λ ranged between 0.916 and 0.996. The relationship between CE_{s2} and λ got stronger as the magnitude of PE decreased.

Applying the scaling methods outlined above, the calculated root mean square values (RMSE) for all four PE rates indicated good agreement between scaled and observed (simulated) results (Table 5). The best results occur at the lowest evaporation rate (0.3 cm d^{-1}), a reflection of having the best r^2 values of all four scenarios. Employing Eq. [5] and [6], that is, using individual scaling factors for all times of interest, for the 0.5 cm d^{-1} evaporation, results are not much different compared with the scaling results using a single scaling factor at t_{ref} (Table 5) according to the respective RMSE values.

Scaling results may be improved if the respective a to d values were used to determine the scaling factors for each time of interest j, rather than a single reference time (Method IB) as follows:

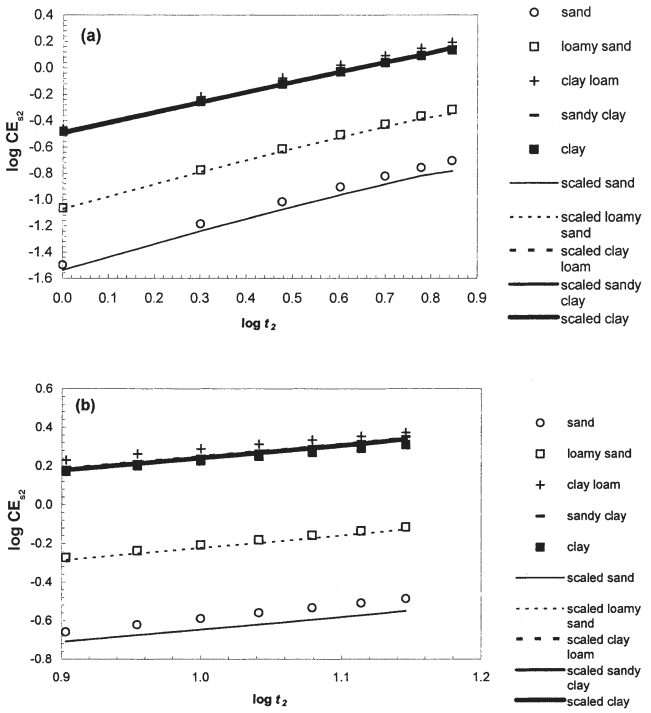

Fig. 5. (a) Log-log plot of simulated (symbols) and scaled (lines) cumulative Stage II evaporation and time for five representative textural-class mean soils for t_2 = 1 to 7 d for a PE of 0.5 cm d^{-1}; and (b) log-log plot of simulated (symbols) and scaled (lines) cumulative Stage II evaporation and time for five representative textural-class mean soils for t_2 = 8 to 14 d for a PE of 0.5 cm d^{-1}.

$$\alpha_{i,j} = \log CE^{e}_{2i,j} - \log CE^{e}_{2\text{ref},j} \quad [7]$$

$$\log CE_{2i,j} = \log CE_{2\text{ref},j} + \alpha_{i,j} \quad [8]$$

Scaled results were compared to modeled results for all times of interest using the time-dependent scaling factors for each PE rate scenario.

Interestingly, we also observed a trend of a log-linear relations between daily CE_{s2} values and PE rates for a fixed λ.

$$\log CE_{s2} = P(PE) + Q \quad [9]$$

where P and Q are empirical coefficients. If measured CE_{s2} values for a reference soil are not available, Eq. [9] can be used to estimate CE_{s2} for any of the 11 mean textural classes and PE rates for each day up to 2 wk on the initiation of Stage II evaporation (Method II). Otherwise, Eq. [9] can be used to get the $CE^{e}_{2\text{ref}}$ value of the reference soil and CE^{e}_{2i} values of any soil needed for Eq. [5] and [7].

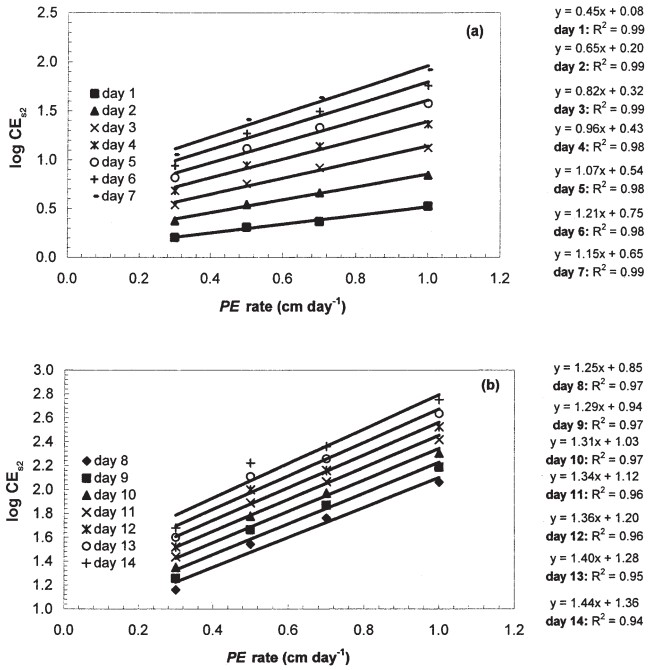

Fig. 6. (a) Log-log plot of CE^{e}_{2i} and PE rates for loam for t_2 = 1 to 7 d according to Eq. [8a]; and (b) log-log plot of CE^{e}_{2i} and PE rates for loam for t_2 = 9 to 14 d according to Eq. [8b].

Following Eq. [9], the log of daily CE_{s2} values for each soil at different PE rates were plotted as shown for loam in Fig. 6. Equation [9] fitted the data very well. Similar high r^2 values were obtained for all PE rates. Because of this strong relation, the slope and intercept values for all soils summarized in Table 6 can be used to estimate CE^{e}_{2i} for any PE rate and any day up to 2 wk on initiation of Stage II evaporation. These CE^{e}_{2i} estimations can be plotted according to each soil's respective λ value as illustrated in Fig. 4a and 4b. Additionally, these CE^{e}_{2i} estimations can be used in the scaling approach outlined above, should the cumulative Stage II evaporation for a reference be unknown.

Evaporation Scaling Comparisons with Experimental Data

To compare with the experimental data, the Stage I cumulative evaporations for three soils (that represented

Table 5. Root mean square errors between observed and scaled cumulative Stage II evaporation (CE_{s2}) values for all four evaporation rates.

Soil textural class	RMSE for 0.3 cm d^{-1} evap.	RMSE for 0.5 cm d^{-1} evap.	RMSE for 0.7 cm d^{-1} evap.	RMSE for 1.0 cm d^{-1} evap.	RMSE for 0.5 cm d^{-1} evap.†
Sand	0.02	0.03	0.04	0.03	0.03
Loamy sand	0.03	0.02	0.02	0.03	0.03
Sandy loam	0.21	0.27	0.33	0.27	0.25
Loam	0.00	0.00	0.00	0.00	0.00
Silty loam	0.22	0.35	0.53	0.44	0.35
Sandy clay loam	0.09	0.18	0.29	0.26	0.18
Clay loam	0.13	0.14	0.28	0.26	0.14
Silty clay loam	0.26	0.36	0.35	0.49	0.37
Sandy clay	0.09	0.05	0.09	0.12	0.05
Silty clay	0.13	0.34	0.50	0.41	0.35
Clay	0.10	0.06	0.02	0.23	0.06

† Scaled using multiple times (Method IB).

Table 6. Slope and intercept (Int) values for linear equations fitted to CE_{s2} results for different soil textures [log CE_{s2} = slope(log λ) + Int].

	Sand		Loamy sand		Sandy loam		Loam		Silty loam		Sandy clay loam	
Day	Slope	Int	Slope	Int	Slope	Int	Slope	Int	Slope	Int	Slope	Int
1	0.042	0.012	0.096	0.037	0.396	0.064	0.446	0.076	0.569	0.066	0.497	0.071
2	0.063	0.035	0.158	0.084	0.629	0.171	0.654	0.201	0.858	0.199	0.752	0.199
3	0.079	0.057	0.207	0.132	0.819	0.278	0.824	0.320	1.102	0.328	0.963	0.322
4	0.091	0.078	0.245	0.178	0.968	0.385	0.960	0.435	1.308	0.454	1.134	0.441
5	0.100	0.994	0.274	0.225	1.081	0.493	1.066	0.545	1.477	0.577	1.271	0.554
6	0.106	0.120	0.294	0.270	1.162	0.602	1.148	0.650	1.617	0.696	1.379	0.663
7	0.109	0.140	0.308	0.314	1.216	0.711	1.209	0.752	1.729	0.811	1.462	0.767
8	0.111	0.160	0.315	0.357	1.245	0.821	1.254	0.849	1.819	0.924	1.525	0.866
9	0.110	0.180	0.319	0.399	1.256	0.931	1.287	0.942	1.892	1.034	1.573	0.961
10	0.109	0.199	0.319	0.439	1.251	1.043	1.314	1.031	1.951	1.141	1.612	1.052
11	0.106	0.218	0.318	0.477	1.234	1.156	1.338	1.117	2.000	1.245	1.645	1.139
12	0.103	0.236	0.317	0.514	1.211	1.270	1.364	1.199	2.045	1.347	1.678	1.221
13	0.101	0.255	0.316	0.548	1.185	1.385	1.397	1.279	2.089	1.447	1.716	1.300
14	0.098	0.273	0.319	0.579	1.160	1.501	1.440	1.355	2.137	1.544	1.763	1.374

	Clay loam		Silty clay loam		Sandy clay		Silty clay		Clay	
Day	Slope	Int	Slope	Int	Slope	Int	Slope	Int	Slope	Int
1	0.503	0.082	0.529	0.084	0.411	0.115	0.559	0.084	0.376	0.128
2	0.730	0.221	0.762	0.234	0.570	0.264	0.799	0.226	0.497	0.288
3	0.918	0.354	0.957	0.377	0.698	0.404	1.006	0.359	0.596	0.435
4	1.073	0.480	1.118	0.512	0.797	0.535	1.182	0.484	0.674	0.570
5	1.198	0.600	1.248	0.642	0.871	0.660	1.332	0.602	0.734	0.696
6	1.299	0.714	1.353	0.765	0.929	0.779	1.459	0.712	0.780	0.811
7	1.380	0.822	1.437	0.884	0.955	0.895	1.568	0.816	0.814	0.919
8	1.445	0.924	1.504	0.998	0.971	1.007	1.662	0.913	0.838	1.020
9	1.500	1.021	1.559	1.108	0.972	1.118	1.745	1.004	0.856	1.115
10	1.549	1.113	1.605	1.215	0.963	1.229	1.821	1.090	0.870	1.206
11	1.596	1.200	1.648	1.319	0.945	1.342	1.893	1.170	0.883	1.293
12	1.647	1.282	1.692	1.420	0.923	1.457	1.967	1.246	0.898	1.377
13	1.706	1.360	1.740	1.520	0.898	1.576	2.045	1.317	0.917	1.460
14	1.778	1.434	1.798	1.619	0.873	1.701	2.131	1.385	0.944	1.543

the range of 11 soils) in the Bonsu (1997) study (sandy loam, sandy clay loam, and sandy clay) were estimated using the parabolic equations fitted to the log-log plots of the CE_{s1} and λ results from the RZWQM simulation at the evaporation rate of 1.0 cm d^{-1} (Eq. [2] and [5]–[8]). The cumulative Stage II evaporation of the test soils was estimated according to the scaling approach (Method I); this method uses Bonsu's (1997) experimental evaporation results for a loam as the reference soil. Method IA using a single reference time according to Eq. [5] and [6], and Method IB using multiple reference times according to Eq. [7] and [8]. Additionally, the cumulative Stage II evaporations for all three soils were estimated using Method II, namely using Eq. [9] for the respective λ value. The estimated and scaled cumulative evaporation using both methods, CE_s ($CE_s = CE_{s1} + CE_{s2}$), were compared with the experimental results.

Using Eq. [1] and the respective coefficient values for 1.0 cm d^{-1}, the cumulative Stage I evaporation values for the three soils of Bonsu (1997) (sandy loam, sandy clay loam, and sandy clay) were estimated. The scaling factor calculations for the three test soils and the subsequent scaling estimates of CE_{s2} were made using Eq. [5] and [6] (Method IA) and Eq. [7] and [8] (Method IB). Method I uses Bonsu's experimental evaporation results for a loam as the reference soil in both Eq. [6] and [8]. Additionally, estimates of CE_{s2} were based on each test soil's respective slope and intercept values summarized in Table 6 and applied to Eq. [9] (Method II). The cumulative Stage I evaporation estimate was added to both CE_{s2} estimates to determine cumulative evaporation. The estimated cumulative evaporation was compared with Bonsu's (1997) experimental results (Fig. 7–9). Good to fair agreement is observed between both methods and experimental data. Deviations between estimated and experimental results may be due to the imperfect log CE_{s2}–log λ relationship; r^2 values closer to unity will yield the best results. There was not much difference between estimates by Method IA and Method IB. However, these methods were better than Method II. Results indicate that having known values for a reference soil helps to estimate and scale values for other soils.

Transpiration Relationships

A quadratic curve (Eq. [3]) fitted the Stage I transpiration, CT_1, for PT = 0.5 cm d^{-1} well (Fig. 10). The results are similar to those for CE_{s1} in Fig. 2. The fitted equation to cumulative Stage I transpiration for different potential transpiration rates can be used to estimate the CT_1 for any soil given the λ value is known.

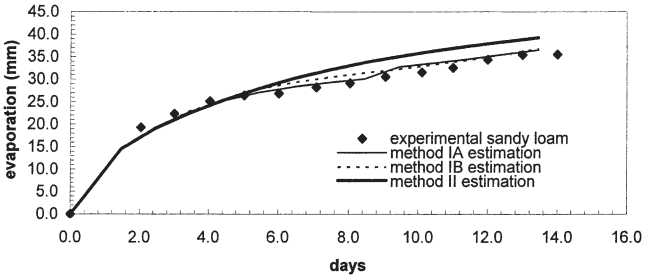

Fig. 7. Plot of estimated (Method I using a reference soil and Method II) and experimental cumulative evaporation of sandy loam at a potential evaporation rate of 1.0 cm d^{-1}.

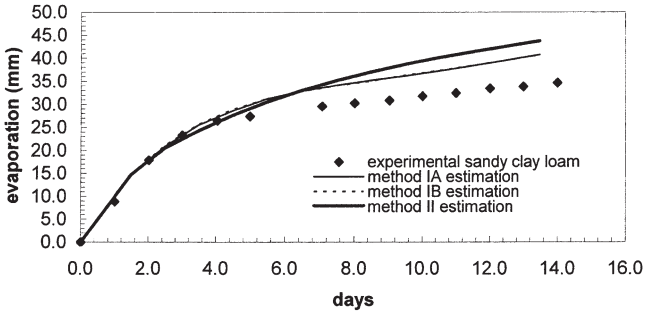

Fig. 8. Plot of estimated (Method I using a reference soil and Method II) and experimental cumulative evaporation of sandy clay loam at a potential evaporation rate of 1.0 cm d^{-1}.

A log-log plot of cumulative Stage II transpiration, CT_2, at different times vs. λ for the same scenario is shown in Fig. 11a and 11b. Here t_2 is the time in days after Stage II transpiration is initiated. (Note: Not all times are shown to avoid confusion; however, all absent times, t_2, were observed to follow the same trend as the times presented.) Again, the cubic equations (Eq. [4]) fitted well to the simulated results of each day for the 14 d after the initiation of Phase II transpiration. The r^2 values got better (closer to unity) with increased time after the initiation of Stage II. As indicated by the high r^2 values (0.81–0.97 for t_2 = 1–7 and 0.97–0.98 for t_2 = 8–14), there is a strong relationship between CT_2 and λ overall.

Transpiration Scaling

The simplification used for scaling cumulative Stage II evaporation was applied to scaling and estimating Stage II transpiration for the 0.5 cm d^{-1} PT rate scenario. For a reference time, t_{ref}, Eq. [9] was used to estimate cumulative Stage II transpiration values for all soils at that time, CT^{e}_{2i}. These estimated cumulative Stage II transpiration values were then compared with the estimated value of a reference soil, CE^{e}_{2i}. The difference between the two variables gives a scaling factor, λ_i, for the respective soil as follows:

$$\beta_i = \log CT^{e}_{2i} - \log CT^{e}_{2\text{ref}} \quad [10]$$

With these scaling factors, estimates of the actual depth of cumulative Stage II transpiration for each soil can be made given that the cumulative Stage II transpiration for the reference soil, CT_{2ref}, is known as follows:

$$\log CT_{2i} = \log CT_{2\text{ref}} + \beta_i \quad [11]$$

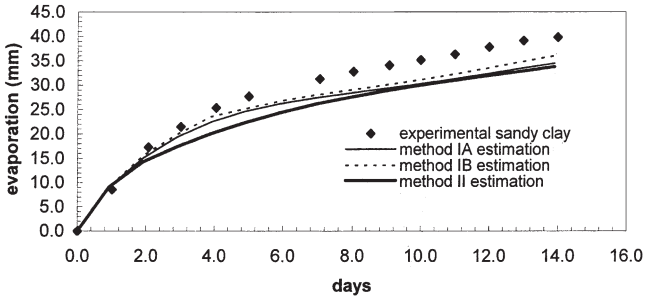

Fig. 9. Plot of estimated (Method I using a reference soil and Method II) and experimental cumulative evaporation of sandy clay at a potential evaporation rate of 1.0 cm d^{-1}.

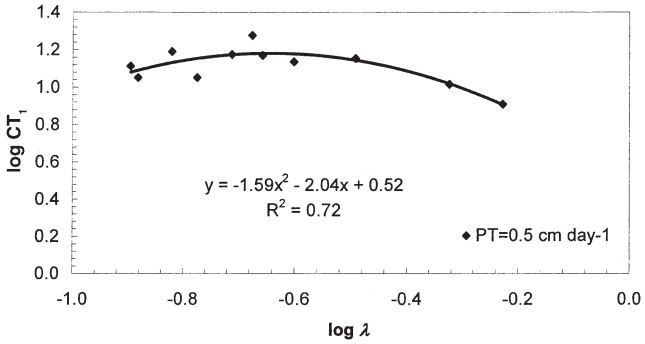

Fig. 10. Log-log relationship of the computed cumulative Stage I transpiration (CT_1) and pore-size distribution index (λ) for the 11 textural-class mean soils for PE = 0.5 cm d^{-1}.

The scaled values calculated for all scenarios through Eq. [11] uses loam as the reference soil, whose λ (=0.220) was close to the mean of all λ values, and a t_{ref} of Day 4 for the 1- to 7-d time span and Day 11 for the 8- to 14-d time span. Five soils were examined (sand, loamy sand, sandy loam, sandy clay, and clay). It should be noted that any soil of known λ can be used as the reference, and any time of interest within the 14-d period can be used as t_{ref}. Much like evaporation, if measured CT_2 values for a reference soil are not available, Eq. [10] can be used to estimate CT_2 for any of the 11 mean textural classes for each day up to 2 wk on the initiation of Stage II evaporation.

Much like the evaporation in Fig. 4a and 4b, it is observed in Fig. 11a and 11b that the CT_2 trend line is

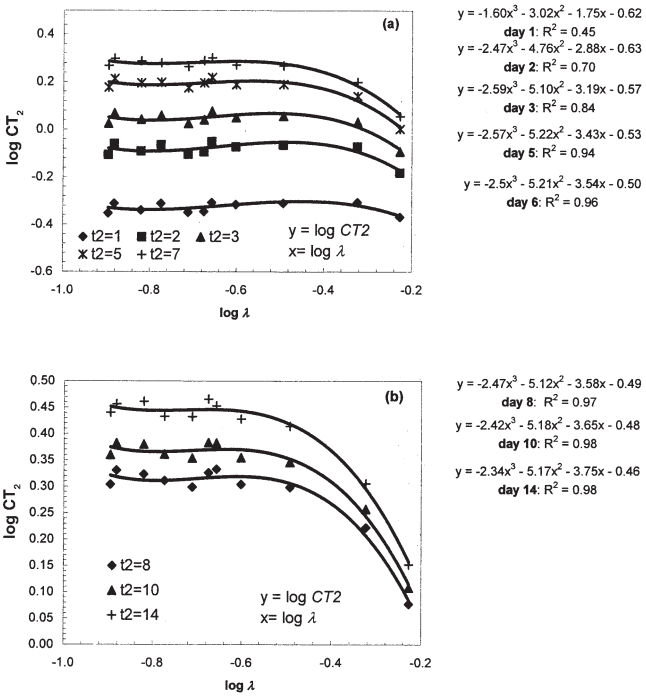

Fig. 11. (a) Log-log relationship of the pore-size distribution index (λ) and computed cumulative Stage II transpiration (CT_2) for the 11 textural-class mean soils for various times, t_2, ranging from 1 to 7 d for a PET of 0.5 cm d^{-1}; and (b) log-log relationship of the pore-size distribution index (λ) and computed cumulative Stage II transpiration (CT_2) for the 11 textural-class mean soils for various times, t_2, ranging from 8 to 14 d for a PET of 0.5 cm d^{-1}.

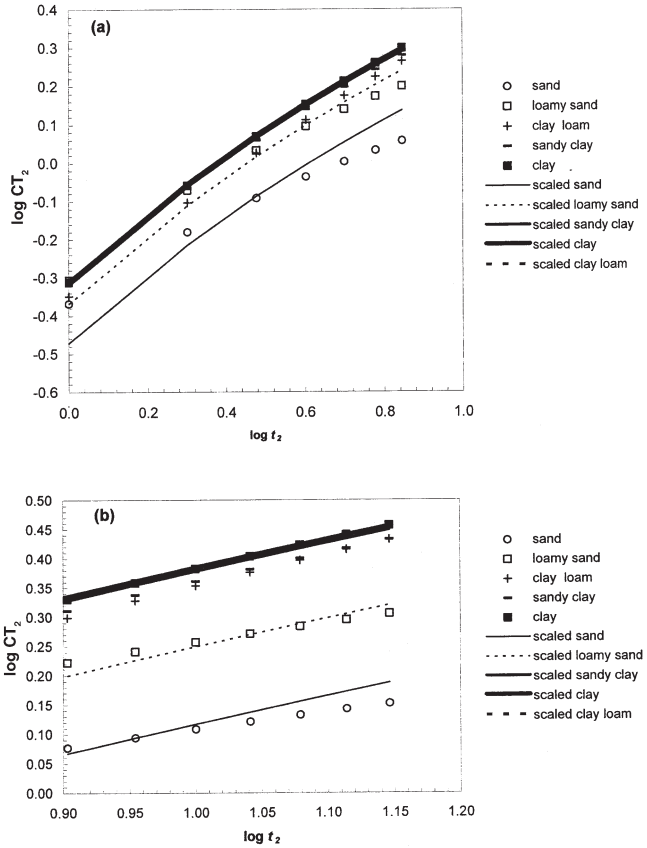

Fig. 12. (a) Log-log plot of simulated (symbols) and scaled (lines) cumulative Stage II transpiration and time for five representative textural-class mean soils for t_2 = 1 to 7 d for a PT of 0.5 cm d^{-1}; and (b) log-log plot of simulated (symbols) and scaled (lines) cumulative Stage II transpiration and time for five representative textural-class mean soils for t_2 = 8 to 14 d for a PT of 0.5 cm d^{-1}.

curvilinear and descends as λ increases. Because of the higher saturated hydraulic conductivities of coarser soils (higher λ values), the soil profile is able to drain quickly leaving less water in the profile and a subsequent lower hydraulic conductivity (Brooks and Corey, 1964) than in finer soils. It is suggested that there is less actual transpiration uptake in a soil profile that has less water available for potential transpiration uptake.

Because the fitted curves in Fig. 11a and 11b are approximately parallel, simulated cumulative Phase II transpiration, CT_2, for five of the soils were compared to the scaled values from Eq. [10] and [11]. Using the 4-d and 11-d mark as the reference times, the empirical coefficients in cubic equations in Fig. 11a and 11b were input into Eq. [9], and the scaling approach outlined in the Materials and Methods section were applied. The scaling results were compared with the simulated values in Fig. 12a and 12b. As can be seen, there is good agreement between the simulated and scaled log values of CT_2 for each soil over time, except for the first 2 d in sand. Scaling estimates improved with time. Discrepancies between the simulated (RZWQM) and scaled (Eq. [10] and [11]) results may be due to low r^2 values from the log CT_2–log λ relationship and approximate nature of the method; r^2 values closer to unity will yield the best results.

SUMMARY AND CONCLUSIONS

In earlier work, it was shown that hydraulic properties of soils as well as the infiltration and redistribution were empirically related to the pore-size distribution index, λ, across soil textural classes. This concept was extended to evaporation and transpiration of near-saturated soils. Cumulative Stage I evaporation, CE_{s1}, for four PE rates and cumulative Stage I transpiration, CT_1, for one PE rate are shown to have a log-log quadratic relationship with λ, while cumulative Stage II evaporation, CE_{s2}, and cumulative Stage II transpiration, CT_2, have a log-log cubic relationship. Coefficients of these empirical relationships for Stage I evaporation are shown to be a function of potential evaporation rates. Additionally, cumulative Stage I evaporation and cumulative Stage II evaporation are shown to also have direct semi-logarithmic relationships with potential rates. To simplify our study, the relationships were for field-saturated soils and would not be applicable for initial shallower wetting depths or initial conditions of lower degrees of saturation. These different initial conditions are of interest and should be examined in future research. However, the relationships of evaporation and transpiration to λ values presented in this paper should serve as a template for those cases.

The empirical coefficients from the λ relationships (Eq. [3] and [10]) were then shown to determine the scaling factors for selected textural classes by a simplified approach (Eq. [4], [5], [11], and [12]). From the evaporation analysis, these empirical coefficients and scaling factors were dependent on evaporation intensity. By applying the soil and scenario specific scaling factors with respect to a middle time and reference soil with a known CE_{s2} or CT_2, values for CE_{s2} or CT_2 for the other major textural classes were estimated (Method I). By this simplified approach, the scaled CE_{s2} or CT_2 were generally in good agreement with the RZWQM simulation results. For CE_{s2}, comparison with experimental data was also good overall. Additionally, semi-logarithmic equations were fitted to the daily CE_{s2} results vs. different potential evaporation rates for each soil and can be used to estimate cumulative Stage II evaporation if reference soil results to apply the scaling method are not available (Method II).

The results presented in this paper are for idealized simple situations, namely under homogeneous and constant potential evaporation or transpiration conditions. Under natural field conditions, soil layering and spatial variability of soil water contents in a soil profile exist, and potential rates vary. Further research is needed to address these complexities, building on the generally encouraging results for simple cases presented here. For example, we may assume that the λ of the top soil (approximately the top 30 cm) controls soil evaporation, whereas a harmonic mean λ of the soil profile controls transpiration. However, for spatial variations and heterogeneities of natural soil horizons, the above estimation and scaling techniques can be used with respect to the dominant soil in each location of a studied area. Hopefully, the finding of this paper and further research will help delineate and quantify spatial variability of soil

water evaporation and transpiration for site-specific management and scaling.

REFERENCES

Ahuja, L.R., J.W. Naney, R.E. Green, and D.R. Nielsen. 1984. Macroporosity to characterize spatial variability of hydraulic conductivity and effects of land management. Soil Sci. Soc. Am. J. 48:699–702.

Ahuja, L.R., J.W. Naney, and R.D. Williams. 1985. Estimating soil water characteristics from simpler properties or limited data. Soil Sci. Soc. Am. J. 49:1100–1105.

Ahuja, L.R., K.W. Rojas, J.D. Hanson, M.J. Shaffer, and L. Ma. 2000. Root Zone Water Quality Model: Modeling management effects on water quality and crop production. Water Resources Publ., Highlands Ranch, CO.

Bonsu, M. 1997. Soil water management implications during the constant rate and the falling rate stages of soil evaporation. Agric. Water Manage. 33:87–97.

Brooks, R.H., and A.T. Corey. 1964. Hydraulic properties of porous media. Hydrological Paper no. 3. Colorado State Univ., Fort Collins.

Campbell, G.S. 1974. A simple method for determining unsaturated conductivity from moisture retention data. Soil Sci. 117:311–314.

Green, R.E., L.R. Ahuja, S.K. Chong, and L.S. Lau. 1982. Water conduction in Hawaii oxic sols. Technol. Rep. 143. Water Resources Research Center, Univ. of Hawaii, Honolulu.

Green, W.H., and G.A. Ampt. 1911. Studies of soil physics: I. Flow of air and water through soils. J. Agric. Sci. 4:1–24.

Gregson, K., D.J. Hector, and M. McGowan. 1987. A one-parameter model for the soil water characteristic. J. Soil Sci. 38:483–486.

Hunt, A.G., and G.W. Gee. 2002. Application of critical analysis to fractal porous media: Comparison with examples from the Hanford site. Adv. Water Resour. 25:129–146.

Kozak, J.A., and L.R. Ahuja. 2005. Scaling of infiltration and redistribution of water across soil textural classes. Soil Sci. Soc. Am. J. 69:816–827.

Ma, L., R. Ahuja, J.C. Aschough, M.J. Shaffer, K.W. Rojas, R.W. Malone, and M.R. Cameira. 2002. Integrating system modeling with field research in agriculture: Applications of the root zone water quality model (RQWQM). Adv. Agron. 71:233–292.

Miller, E.E., and R.D. Miller. 1956. Physical theory for capillary flow phenomena. J. Appl. Phys. 27:324–332.

Nielsen, D.R., J.W. Hopmans, and K. Reichardt. 1998. An Emerging technology for scaling field soil–water behavior. *In* Scale dependence and scale invariance in hydrology. Cambridge Univ. Press, Cambridge, UK.

Nimah, M., and R.J. Hanks. 1974. Model for estimating soil–water–plant–atmospheric interrelation: I. Description and sensitivity. Soil Sci. Soc. Am. Proc. 37:522–527.

Pachepsky, Y.A., D.E. Radcliffe, and H.M. Selim. (ed.) 2003. Scaling methods in soil physics. CRC Press, Boca Raton, FL.

Peck, A.J., R.J. Luxmoore, and J.L. Stolzy. 1977. Effect of spatial variability of soil hydraulic properties in water budget modeling. Water Resour. Res. 13:348–353.

Rawls, W.J., D.L. Brakensiek, and K.E. Saxton. 1982. Estimation of soil water properties. Trans. ASAE 25:1315–1320.

Rieu, M., and G. Sposito. 1991. Fractal fragmentation, soil porosity, and soil water properties. I. Theory. Soil Sci. Soc. Am. J. 55:1231–1238.

Ritchie, J.T. 1972. Model for predicting evaporation from a row crop with incomplete cover. Water Resour. Res. 8:1204–1213.

Russo, D., and E. Bresler. 1980. Scaling soil hydraulic properties of a heterogeneous field. Soil Sci. Soc. Am. J. 44:681–683.

Sharma, M.L., G.A. Gander, and C.G. Hunt. 1980. Spatial variability of infiltration in a watershed. J. Hydrol. (Amsterdam) 45:101–122.

Sharma, M.L., and R.J. Luxmoore. 1979. Soil spatial variability and its consequences on simulated water balance. Water Resour. Res. 15:1567–1573.

Shuttleworth, W.J., and J.S. Wallace. 1985. Evaporation from sparse crops: An energy combination theory. Q. J. R. Meteorol. Soc. 111: 839–855.

Simmons, C.S., D.R. Nielsen, and J.W. Biggar. 1979. Scaling of field-measured soil water properties. Hilgardia 47:77–154.

Tillotson, P.M., and D.R. Nielsen. 1984. Scale factors in soil science. Soil Sci. Soc. Am. J. 48:953–959.

Tyler, S.W., and S.W. Wheatcraft. 1990. Fractal processes in soil water retention. Water Resour. Res. 26:1047–1054.

Warrick, A.W., and A. Amoozegar-Fard. 1979. Infiltration and drainage calculations using spatially scaled hydraulic properties. Water Resour. Res. 15:1116–1120.

Warrick, A.W., G.M. Mullen, and D.R. Nielsen. 1977. Scaling field-measured soil hydraulic properties using a similar-media concept. Water Resour. Res. 13:355–362.

Williams, R.D., and L.R. Ahuja. 1991. Estimating soil water characteristics using physical properties and limited data. *In* M.Th. van Genuchten (ed.) Indirect methods for estimating the hydraulic properties of unsaturated soils. Proc. Int. Works, Riverside, CA. 11–14 Oct. 1989. Univ. of Calif. Press, Riverside.

Williams, R.D., and R.D. Ahuja. 2003. Scaling and estimating the soil water characteristic using a one-parameter model. p. 35–48. *In* Scaling methods in soil physics. CRC Press, London.